CrossMark

Sunspot Numbers from ISOON: A Ten-Year Data Analysis

K.S. Balasubramaniam[1] · T.W. Henry[2]

Abstract Sunspot numbers are important tracers of historical solar activity. They are important in predicting the oncoming solar maximum, in the design of lifetimes of space assets, and in assessing the extent of solar-radiation impact on the space environment. Historically, sunspot numbers have been obtained visually from sunspot drawings. The availability of digital images from the US Air Force Improved Solar Optical Observing Network (ISOON) prototype telescope concurrent to observer-dependent sunspot numbers recorded at the National Solar Observatory (NSO) has provided a basis for comparing sunspot numbers determined from the two methods. We compare sunspot numbers from visual and digital methods observed nearly simultaneously. The advantages of digital imagery are illustrated.

Keywords Sunspots · Solar cycle · Sunspot numbers

1. Introduction

The temporal fluctuation of the daily sunspot numbers is the underlying basis for understanding and modeling the historical nature of solar activity, which in turn drives the prediction of solar cycles (*e.g.* Hathaway, Wilson, and Reichman, 1999; Hathaway, 2010). Counting sunspots is fraught with inaccuracies (see, *e.g.*, Hoyt, Schatten, and Nesme-Ribes, 1994; Cliver, Clette, and Svalgaard, 2013). A complex system of *consistency factors* continues to drive the determination of the scaled international sunspot index $[R]$. These factors include telescope optical quality, resolution, atmospheric seeing, photometric sky quality, and observer vision. They have changed over time because sunspot observing is a human activity. Hence, attempts to normalize our measurements of sunspot activity that are obtained over

---

✉ K.S. Balasubramaniam
ks.bala@yahoo.com

[1] Air Force Research Laboratory, Space Vehicles Directorate, Kirtland AFB, NM, USA

[2] Boston College at Air Force Research Laboratory, Kirtland AFB, NM, USA

decades and centuries from different data sources lead to unintended errors. In addition, determining the boundary of a sunspot region and to which region the observed sunspot or pore belongs has led to questioning the authenticity of the very definition of a sunspot index. However, despite the absence of consistent and verifiable data, it is vital to capture a model variation of the solar cycle over centuries. The international sunspot number is the most viable measure of inference to represent solar cycles. We refer to the body of work that is captured in the series of Sunspot Number Workshops organized by Cliver, Clete, and Svalgaard (ssnworkshop.wikia.com/wiki/Home) to help understand the difficulties of reconciling sunspot numbers.

The solar-physics literature has numerous references to a rich tradition of research efforts to compare sunspot numbers from various observatories. This is illustrated by additional efforts that were made to include sunspot-number recordings from digital and historic data. They include measures from the Debrecen Solar Observatory (Győri, Baranyi, and Ludmány, 2010), Kanzelhöhe Observatory (Pötzi *et al.*, 2016), Kislovodsk (Tlatov *et al.*, 2014), and Kodaikanal (Sivaraman, Gupta, and Howard, 1993).

1.1. Sac Peak White-Light Telescope

Historically, observers at the National Solar Observatory (NSO) and its predecessor, the Sacramento Peak Observatory, have kept daily records of sunspot number $[R]$ made from hand-drawings from 1953 – 2006. A 15 cm telescope projected a white-light image (no filters) on a whiteboard using an eyepiece to form a 19 cm image. The eyepiece was manually adjusted every day to fill the visually focused solar image so that the visual limb was enclosed by the 19 cm circle (see: nsosp.nso.edu/node/16). The sunspot number $[R]$ (also known as the Wolf number or the International Sunspot Number, ISN) is defined by

$$R = k(10g + f), \tag{1}$$

where k is an observatory-dependent factor, g is the number of groups, and f is the number of individual spots observed. For Sacramento Peak images, k was always assigned a value of unity for unknown historical reasons.

These indices and the corresponding daily drawings were transmitted to the NOAA Space Weather Prediction Center and its predecessor at Boulder, CO, USA to contribute to the international sunspot number.

1.2. ISOON Telescope

A partially overlapping and nearly decade-long (2002 – 2011) digital effort to capture a consistent verifiable measure of the sunspot index was made using the Improved Solar Observing Optical Network (ISOON) prototype telescope operated at the NSO at Sunspot, New Mexico, USA, by the Air Force Research Laboratories.

The ISOON telescope is a 25 cm aperture polar-axis evacuated refractor with a 5000 mm primary focal length. The spectral filters consisted of 150 mm aperture dual Fabry–Perot filters with a bandpass of 0.1 Å at 6303.15 Å, a region of the solar spectral pure continuum that is devoid of any spectral line. The detector was a 2048×2048 pixel water-cooled XEDAR CCD camera with 4096 gray levels. Continuum images at an angular resolution of $1.1''$ per pixel were acquired at a cadence of five minutes. The raw images were scaled to a solar radius of 890.4 pixels and de-rotated by the solar position angle: P_0 (Neidig *et al.*, 1998; Balasubramaniam and Pevtsov, 2011).

One of us (author T.W. Henry) was the same observer who compared the sunspot groups from both hand-made drawings and the digital images for a year and a half during 2003 – 2004 from these two different instruments. This article describes the insights gained from the comparison of ISOON data with historic Sacramento Peak sunspot data.

In Section 2 we describe the data from the individual instruments and intercompare the individual measures. In Section 3 we describe the insights gained from analyzing the long- and short-term variations.

2. The Data

In 2003 – 2004 a 17-month study was conducted comparing hand drawings from the NSO's white-light telescope with ISOON continuum images. The observing sites were approximately 100 feet apart.

2.1. Historic Sunspot Data

At the 15 cm telescope, equipped with a projection board, observers sketch a sunspot drawing on a sheet of paper on which the white-light Sun is focused. Sunspots are drawn with a pencil. The paper is usually of high quality so as not to confuse dark flaws in the paper with solar features or sunspots. Typically, penumbrae are drawn with a sharp pencil, while umbrae are drawn and filled in. A second piece of paper may be waved in the light path in front of the drawing to ensure a particular dark feature being projected is actually of solar origin. White-light faculae may also be added to the drawing. In the next step, the sheet is removed from the projection board, groups are marked, the Wolf number is computed, labels are added, and the drawing is complete. An example of a sunspot-number drawing is shown in Figure 1. The results from the (hand-drawn) sunspot number were sent to NOAA daily since 1953, although the data-accumulation process started in 1948. The data were sent by facsimile. (We note that this method of sunspot counting is the basis for sunspot-number measures used by USAF's Solar Electro-optical Network, whose data from the Solar Observing Optical Network (SOON) are transmitted to NOAA and then to the World Data Center for Solar Terrestrial Physics, which helps in reconciling international sunspot numbers.)
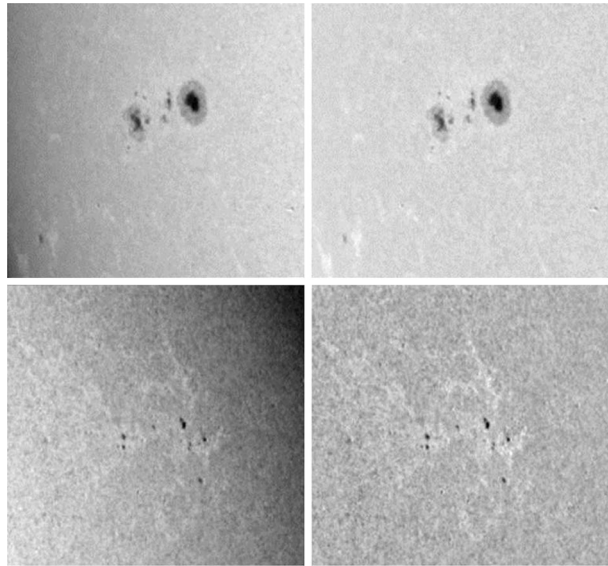
The method used to count sunspots at the NSO was handed down from observer to observer. Each umbra was counted as a separate spot; a penumbra without an umbra is neglected when present within a spot group that has a different umbra to contrast with. If a separate penumbra from a region on the limb can be identified that is not a part of any other spot group, then that is counted as a spot group. Typically, the drawing was compared to a NOAA Solar Region Summary to separate and determine the number of groups when labels were applied.

2.2. Digital Data from ISOON

When the USAF's ISOON prototype was constructed, the ability to make automated measurements of true continuum images was incorporated into the system (Neidig *et al.*, 1998; Balasubramaniam and Pevtsov, 2011). The method is as follows: i) the solar-disk image is corrected for atmospheric and optical distortions and is made circular. ii) A radial averaging function is used to remove penumbrae, spots, and faculae. We used the criteria that the local intensity (averaged to unity) is between 0.92 – 1.08 to define the quiet-Sun radial profile

Figure 1 Left: sunspot drawing used to record sunspot numbers for 06 January 2004 using the NSO telescope at the Hilltop Dome. There are 3 sunspot groups and 19 spots, resulting in an *R*-number of 49. Right: the corresponding digital image from ISOON. The *R*-number is 50. We note that the E- and W-directions are flipped in the two drawings. The original sunspot drawing is as observed.

using a polynomial fit. iii) A 2D limb-darkening function is reconstructed. (Tests of the limb-darkening accuracy have been verified over a few thousand images.) iv) The limb-darkening function is subtracted from the solar-disk image. Removal of limb darkening helps to identify individual smaller spots that might otherwise be missed, and to identify the location of faculae with better visual contrast. The resulting image is also used to calculate irradiance deficit. (The quiet-Sun solar disk has an approximate value of unity, with embedded granular contrast variations accounting for the fluctuations.) v) Contiguous penumbral areas are identified where the local intensity is below 0.92, and umbral areas are identified, whose local intensity is below 0.68.

We elaborate on how we identified the sunspots on an image that was corrected for limb-darkening effects. Three simultaneous criteria are used to determine a feature (umbra or penumbra). The criteria are based on intensity, area, and temporal continuity as follows:

a) Intensity: The normalized intensity values of 0.92 and 0.68 as cutoffs were determined by using intensity distributions in a histogram. By examining the inflection points in a histogram, we determined the intensity cutoffs. The details of this technique are similar to that applied by Balasubramaniam (2002). The consistency of the cutoffs was determined by examining the cutoff application to identifying umbral and penumbral boundaries with ISOON data that were obtained for a year in 2003.

b) Area: A feature (umbra or penumbra) area was determined by the following method, adapted from Smith and Smith (1963) and reported by Henry (2015). A pixel on the image (1.1″ square) defines a grid unit. The solar radius [*r*] in each image is 890.43 pixels. A contouring algorithm determines the boundary of a feature within the solar image. The vertices of the boundary are used to measure the area it encloses, in grid units. The true

Figure 2 Top left: east-limb example: a continuum image on the east limb with limb-darkening. Top right: the same region as the top-left image without limb darkening. Bottom: west-limb example: similar to top figures with and without limb darkening. The images are $\approx 240 \times 290$ arcseconds.

area, in micro-hemispheres, is given by

$$A = A_{c} \frac{10^{-6}}{A_{s}}. \tag{2}$$

Here A_{c} is the area of the feature and A_{s} is the area of the Sun, in grid units. The exponent refers to the micro-hemisphere. By trial and error, we determined that the number of vertices has to be at least 12 to eliminate noise and dust spots in the image. The smallest unit area measured is one solar micro-hemisphere.

c) Temporal continuity: For a feature (umbra and/or penumbra) to be recognized automatically, it has to be present in three consecutive images. Since the cadence of each image is at every five minutes, the image has to be present for at least 15 minutes. This eliminates granular lanes, dust, and short-lived pores. The continuity is determined by projecting the contours of each image onto the contours of the next image. If the two contours overlap, the feature is counted.

Images were examined visually for transient dust specks or shadows. The groupings of active regions were manually delineated against the current day's NOAA region-summary report, issued at 00 UT. The resulting images were then fed into an algorithm to measure sunspot numbers, umbral and penumbral areas, and irradiance measures (Neidig and Henry, 2004). Human intervention was necessary to allow for a visual recognition of what constituted the assignment of pores to an active region, potential specks of transient dust, and errors due to automated flat-fielding of CCD images when clouds interfered with the acquisition of flat-fields. The right-hand side of Figure 1 illustrates a comparative digital image.

It is important to note that the digital images were corrected for dark-current residuals and flat-fielding effects. In addition, to normalize the intensity of sunspot features regardless of where they are on the disk, the images were limb-darkening corrected (*cf.* Figure 2). Even on the digital images, spot-groups were visually identified against NOAA group numbers, and where NOAA numbers did not exist, they were assigned a temporary region number. The automated program recognizes the contours, counts, and locations of all penumbrae and

Figure 3 A composite solar image on 14 February 2004, corrected for limb-darkening, with labels and arrows showing the corresponding solar regions, similar to a projection drawing.
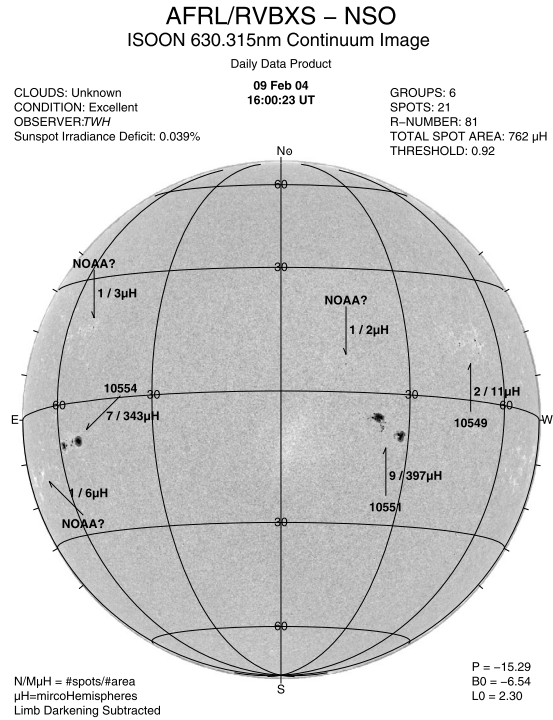
umbrae based on thresholds discussed above. The resulting image is also used to calculate the irradiance deficit, the relative darkness of spots, and the areas of sunspot penumbra and the umbra.

The system is designed to take the NOAA Region Summaries and provide a sunspot-number count automatically, as is shown in Figure 3. The labeling is sometimes altered manually to prevent overlap or visual distractions. The data-processing algorithm can obtain sunspot-number counts and irradiance deficit whether an operator is present or not. However, human intervention is necessary when sunspot groups split or new groups appear in the vicinity of older groups, or labels appear to overlap, which causes confusion upon a visual examination. Even seeing conditions are measurable from the image quality. When it is initiated, the algorithm runs continuously, providing Wolf number, area, irradiance deficit, and an equivalent drawing without further intervention.

2.3. Comparing Hand-Drawings with Imagery

An important part of transitioning from a 52-year hand-drawn database to a digital form was to ensure the consistency of the digital data overlap with the hand-drawn data. Table 1 shows the results of measurements from sunspot drawings and ISOON imagery for the start of the comparison in 2003. This comparison was continued until 11 May 2004. NSO hand-drawings were permanently discontinued after this date, driven by programmatic decisions. Table 1 in itself does not show the smaller pores, but the digital imager detects smaller and fainter penumbrae and pores that are reflected in the G-number, whereas the drawing identifies more individual umbrae, as reflected in spot-counts. An immediate conclusion from this analysis is that a visual observer easily misses fine spots and spot groups, particularly near

Table 1 Direct comparison of spot count R-number from ISOON (first letter I denotes image) and drawing (first letter D denotes drawing). The date designations are apparent. For ISOON digital images, IN, IR, IG, IA, and IQ represent the number of individual spots, sunspot number, group number, area (micro-hemispheres), and image quality (good, excellent, fair, or poor), respectively. DT is the time difference between a digital image and a drawing, in minutes. For the drawing images, DN, DR, DG, and DQ represent the number of individual spots, sunspot number, group number, and seeing quality (excellent, good, fair, or poor), respectively. Since the same observer (author T.W. Henry) had to record both data, the time difference between the two processes is shown in the column DT. The group number IG is determined by $12.08 \times$ number of groups (see Hoyt and Schatten, 1998).

| DD	MON	YYYY	IN	IR	IG	IA	IQ	DT	DN	DR	DG	DQ
7	Jan	2003	29	99	85	925	G	−90	59	109	60	G
13	Jan	2003	35	135	121	1149	E	−2	56	136	97	E
16	Jan	2003	14	114	121	661	G	39	13	93	97	P
22	Jan	2003	15	85	85	463	G	9	20	80	72	G
24	Jan	2003	19	79	72	663	F	8	24	84	72	F
27	Jan	2003	19	99	97	417	G	3	19	79	72	F
28	Jan	2003	19	99	97	483	F	4	22	102	97	F
29	Jan	2003	21	81	72	509	G	−58	23	83	72	P
30	Jan	2003	10	70	72	265	F	−3	14	64	60	F
31	Jan	1003	5	45	48	170	F	20	7	47	48	F
3	Feb	2003	10	30	24	475	F	−1	18	38	24	F
6	Feb	2003	23	83	72	375	G	13	19	69	60	F
7	Feb	2003	23	93	85	333	G	3	29	99	85	G
10	Feb	2003	15	85	85	284	G	−8	19	89	85	F
19	Feb	2003	8	38	36	407	F/G	4	10	40	36	F
27	Feb	2003	5	35	36	196	E	−25	6	36	36	G
28	Feb	2003	6	36	36	610	E	−36	8	38	36	E
3	Mar	2003	17	87	85	913	G	−13	16	56	48	F
6	Mar	2003	14	64	60	695	F/G	4	13	53	48	G

the limb. Equation (1) has a group factor of 10, and hence finding additional smaller sunspot groups increases the sunspot number $[R]$ by at least 11 counts per group. We note that seeing affects the counting. If poorer seeing blurs the existence of spots, then the numbers are lower, similar to a visual observer losing sunspot counts. This poses a difficulty in reconciling older sunspot numbers from across multiple telescopes that are observer-dependent when bringing them to the modern digital age. The advantage of the digital technique is that since data are preserved, the authenticity of the sunspot counts can be verified, which is not possible for the hand-drawn sunspot-drawing records.

## 2.4. Comparing ISOON Measures to International Sunspot Numbers

It is important to compare the measures of ISOON sunspot numbers to the ISN (www.sidc. be/silso/datafiles), which serve as historical reference data. We compare the two sunspot numbers as shown in Figure 4. The updated ISN numbers (corrected since July 2015) are higher by a factor of ≈ 1.3 than the corresponding numbers as recorded by ISOON. The correlation coefficient is of ≈ 0.95 between the two data sets for the time period investigated.

A high ($\approx 95\%$) correlation between the two numbers shows the high confidence that we must attribute to the international sunspot numbers when digital data were historically

Figure 4 The International
Sunspot Number *versus* the
ISOON *R*-number during the
study period described in the text.
The data are plotted only on days
when ISOON digital imagery
were available.
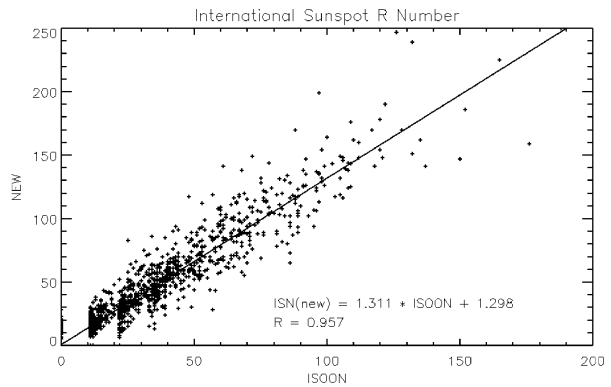
Figure 5 A nearly decade-long
comparison of new ISN to
ISOON measures, as a difference
of the two measures. The
continuous line shows a monthly
average and the dotted points are
the individual numbers. The ISN
overestimates the number of
sunspots during high solar
activity years.
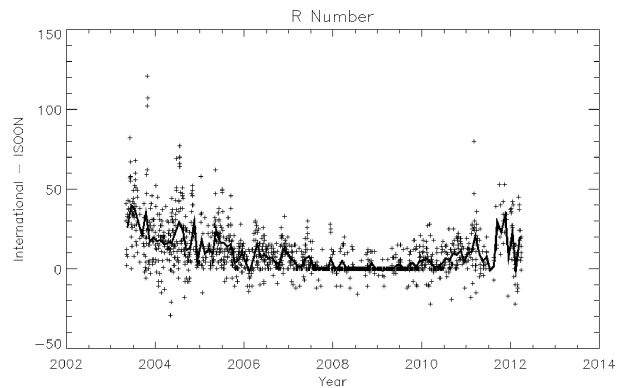
absent. The curve provides an opportunity to revert digital numbers to international numbers
using the linear equation

$$R_{\text{Int}} = k R_{\text{ISOON}} + B, \tag{3}$$

where $k = 1.3$ for the comparison period (May 2003 – March 2012). To understand the ex-
tent of the differences between ISOON and ISN during nearly a decade (2002 to 2011), we
show the actual differences in Figure 5. During high solar activity, ISN systematically over-
estimates the number of sunspots. These spots are particularly noticeable around solar max-
ima years in 2004 and 2012. This immediately leads to a consideration of how the K-factor
(an annual reconciliation index) varies with time. Table 2 shows the annual variation of the
K-factor (see Equation (3)). The solar-maximum periods show a high correlation, while the
solar minimum shows a relatively weaker (still high) correlation. The reason is that dur-
ing times of minimal solar activity, one observatory might see a short-lived pore (counted),
whereas another observatory will not report this. For example, on 13 October 2003, two
pores in the southwest quadrant were observed late in the afternoon and were counted as
one spot group. On 14 October, there were three pores (in two different groups) seen for a
short period of time. The ISOON data did not detect any spots (because of intensity thresh-
olds; the spots were too small or too faint) in the morning on either day, where the images
show no pores on the disk. The ten-year mean correlation coefficient is high because there
are a disproportionate number of points (422 days) during which there were no sunspots

Table 2 Yearly straight-line least-square fits of the International R-number to the ISOON R-number. M is the slope, B the intercept, R the correlation coefficient, and NP is the number of points in each year. The ten-year mean correlation coefficient is high because there are a disproportionate number of points (422 days) during which there were no sunspots during the solar minimum.

Year	M (slope)	B (intercept)	R (correlation)	NP (# points)
2003	1.259	10.036	0.920	118
2004	1.288	5.580	0.878	209
2005	1.276	3.984	0.912	98
2006	1.199	3.330	0.917	188
2007	1.254	0.853	0.918	98
2008	1.121	0.524	0.898	211
2009	1.115	0.844	0.866	195
2010	1.082	3.990	0.879	161
2011	1.181	4.928	0.921	85
2012	1.198	2.246	0.847	44
ALL	1.311	1.298	0.957	1606

during the solar minimum. These results show the subtleties of sunspot counts from figure drawings when compared to digital data.

Despite the high correlation, another source of difference is that while the ISOON number is determined from a "snapshot" of the Sun taken over 15 minutes, the ISN numbers are reconciled from data obtained by about 20 observatories from a 24-hour period. This causes differences that are due to either counting short-lived spots during ISOON observations or completely missing them, which was accounted for by the ISN data.

Uncertainties might be contributed to the International Sunspot Number counts by transient spots (with lifetimes of a few hours) during a time when an observer records visual sunspots by drawing them. These are not traceable either. The advantage of digital data is the potential of studying the temporal evolution of sunspot numbers for a particular active region, which can provide additional insights into the evolution of solar activity within short periods of time. This correlation demonstrates that there needs to be an additional reconciliation factor of the new ISN that is a function of solar cycle phase.

## 2.5. Comparing Pre-2015 ISN to Post-2015 ISN to ISOON Measurements

The Sunspot Index and Long-term Solar Observations website at the Royal Observatory of Belgium (www.sidc.be/silso/datafiles) changed the original ISN series (version 1.0; also referred to as "OLD") to a new ISN series (version 2.0; referred to as "NEW"). We reported here the comparison of digitally derived ISOON Sunspot Numbers with the new series, 2.0 so far. From the point of view of ISOON data, it will be useful to compare the difference between the OLD and the NEW ISN values. To help us understand this difference, we plot it in Figure 6. The figure clearly shows that there is a continued nonlinear trend that increases with the solar cycle. We recall that the ISN numbers (OLD or NEW) are reconciled from a large number of observatories around the world. In comparison to ISOON, the OLD ISN numbers underestimate the spot count, while the NEW ISN numbers overestimate the spot count (Figure 5). The overestimation or underestimation of ISN varies with the strength of the solar cycle (Figure 6). The correlation coefficients have changed insignificantly, regardless of the sources of the ISN. They are 0.956 for ISOON number *versus* OLD and 0.957 for ISOON number *versus* NEW ISN.

The insignificance of the difference between OLD or NEW ISN numbers when compared to ISOON numbers during 2002 – 2012 is further illustrated in Figure 7, where we depict

Figure 6 Difference between
NEW ISN and OLD ISN (see
text) during the period of ISOON
observations.
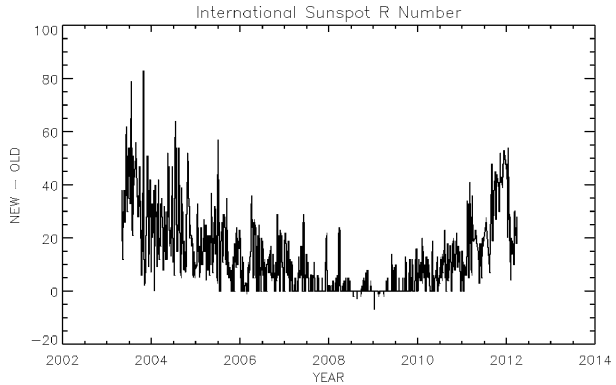
Figure 7 Scatter plot of the
difference between NEW ISN
and OLD ISN and ISOON
number counts during the period
of ISOON observations
(2002–2012) (see text).
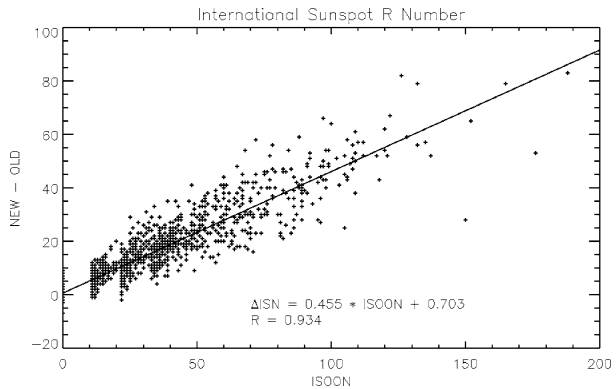
a scatter plot of the difference, referenced against the ISOON number count. Here we see
once again that the difference in the sunspot counts is greater during higher solar activity or
for larger sunspot numbers.

2.6. Reduced Irradiance due to Sunspot Blocking

An additional advantage of digital imagery is that the reduction in continuum intensity due
to the blocking of sunspots can be measured (Neidig and Henry, 2004). The reduction, or
deficit [f_λ], in irradiance due to a dark feature with area A [pixels^2] and intensity I_λ is

$$f_\lambda = 6.18 \times 10^{15} \, \text{cm}^2 \, \text{pix}^{-2} \big(I_\lambda(0)/600 \big) I_\lambda \, \text{d}A/(1 \, \text{AU})^2 \, \text{erg s}^{-1} \, \text{cm}^{-2} \, \text{Å}^{-1}, \qquad (4)$$

where $I_\lambda(0)$ is the intensity of the quiet Sun at disk center, averaged over an area of
110 arcseconds squared (100 × 100 pixels). We note that I_λ will appear as a nega-
tive number in the ISOON reductions. For $\lambda = 6303.15$ Å, $I_\lambda(0) = I_\lambda/0.83 = 3.036 \times$
$10^6 \, \text{erg s}^{-1} \text{Å}^{-1} \, \text{cm}^{-2} \, \text{sr}^{-1}$ (Allen, 1991). The intensity [I] here is taken from a limb-
darkening subtracted image. The number 600 arises because ISOON's data camera acqui-
sition system sets the disk-center intensity to 600 counts as a reference. Figure 8 shows
the irradiance reduction derived from ISOON data (2003–2011; 1532 days of observing)
compared to the sunspot area as determined by the thresholds mentioned previously. The
linearity between the two quantities is notable. Sunspot areas or irradiance-deficit measures
might be a quantitative measure of the solar-activity cycle.

Figure 8 Irradiance reduction in sunspots compared to the area. We note the high correlation and proportionality. Extremes in the data such as the 2003 Halloween sunspots (28 – 29 October 2003) are in the top-right corner. The area measure accounts for foreshortening, while the irradiance measure has no such correction by definition.
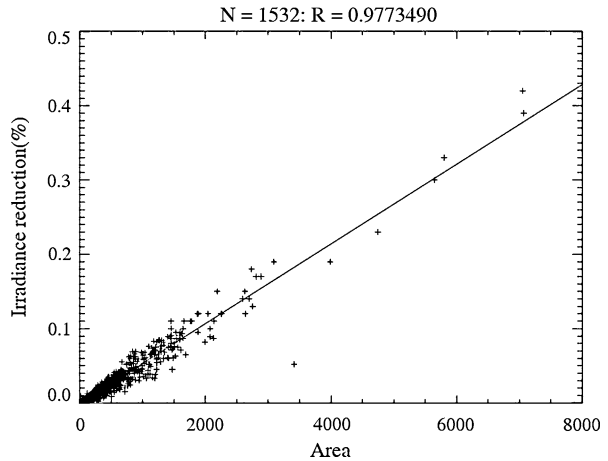
3. Temporal Variations of Sunspot number, Area, and Irradiance Deficit

3.1. Long-Term Variations

After establishing the basis of the digital measures of sunspot number, area (in millionths of the solar hemisphere), and irradiance deficit, we next explore the temporal variations for 2003 – 2010. Figure 9 shows the solar-cycle dependence of the sunspot number, sunspot area (penumbral area + umbral area), and the irradiance deficit. Within each plot an inset shows the 30-day data before 09 April 2010. The label "current day" in the plot indicates that this display can be updated at any given time when new observations accumulate. The solar-cycle behavior is evident in the comparison, which starts in 2003 at the end of the maximum in Cycle 23 and ends in 2010 at the beginning of the new Cycle 24. The sunspot number is loosely correlated with sunspot area. The clarity of the sunspot area increases, and the corresponding increase of the irradiance deficit during the end of October 2003 is evident. At this time, the Sun was exceptionally densely covered with a large number of sunspots. Similarly, the insets show the 28-day sunspot rotation off the solar disk and the dramatic changes in sunspot area and irradiance deficit during late March to early April 2010.

3.2. Intra-day, Short-Term Fluctuations of Sunspot Component Areas During Flares

In an attempt to understand the short-term variations of these quantities' influence and to help attribute the underlying physics to these changes, it is instructive to determine the change in sunspot component areas (namely umbra and penumbra) within a day, particularly when a solar flare occurs. With the availability of consistent high-resolution digital data at a far higher cadence (one minute or higher), the contrast of intra-day changes compared to daily changes becomes clear. Figure 10 illustrates the intra-day changes. The panels in Figure 10 show the X6.5 flare of AR 10930 on 06 December 2006. The mean Hα intensity for the flare, averaged over the active region, is shown in the top right panel to help in identifying the start of the flare (vertical line). This figure illustrates that intra-day changes in sunspot activity are well captured by area and intensity changes, and not by sunspot number measures. This is possible through the high-quality digital images.
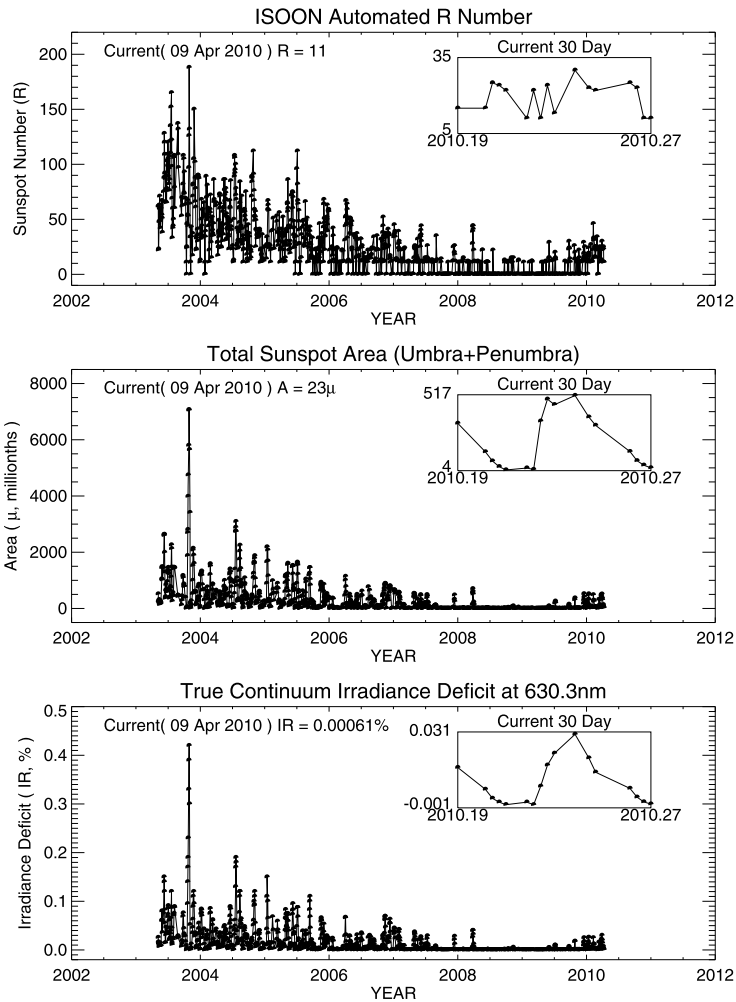
Figure 9 Automated Sunspot Number [R], sunspot areas, and irradiance reductions from 2003 – 2009. The inset in each plot demonstrates the 30-day variations before each of the quantities, reckoned from the current day (which in this case was 09 April 2010).

The complexity of sunspot dynamics can be represented by changes in the umbral and penumbral intensities and areas. For reference, the relative Hα light curves of the activity are plotted. The Hα light-curve intensities are relative to a quiet-Sun solar chromosphere at the disk center. The Hα light curve is a measure of the chromospheric activity, similar to the GOES X-ray light curves, except that Hα measures the changes in activity in individual active regions. The mean umbral and penumbral continuum intensities are derived after the umbra and penumbra are delineated by a contoured threshold as described above. The umbral and penumbral areas are distinct and plotted in units of millionths of the solar hemisphere. The vertical lines in the figure show the start of the solar flare times for the active region as documented by the NOAA Solar Activity Summaries. For example, after the 06 December 2006 X6.5 flare, the umbral areas decrease and the penumbral areas increase. A possible interpretation is that the horizontal penumbra fields have relaxed and resulted
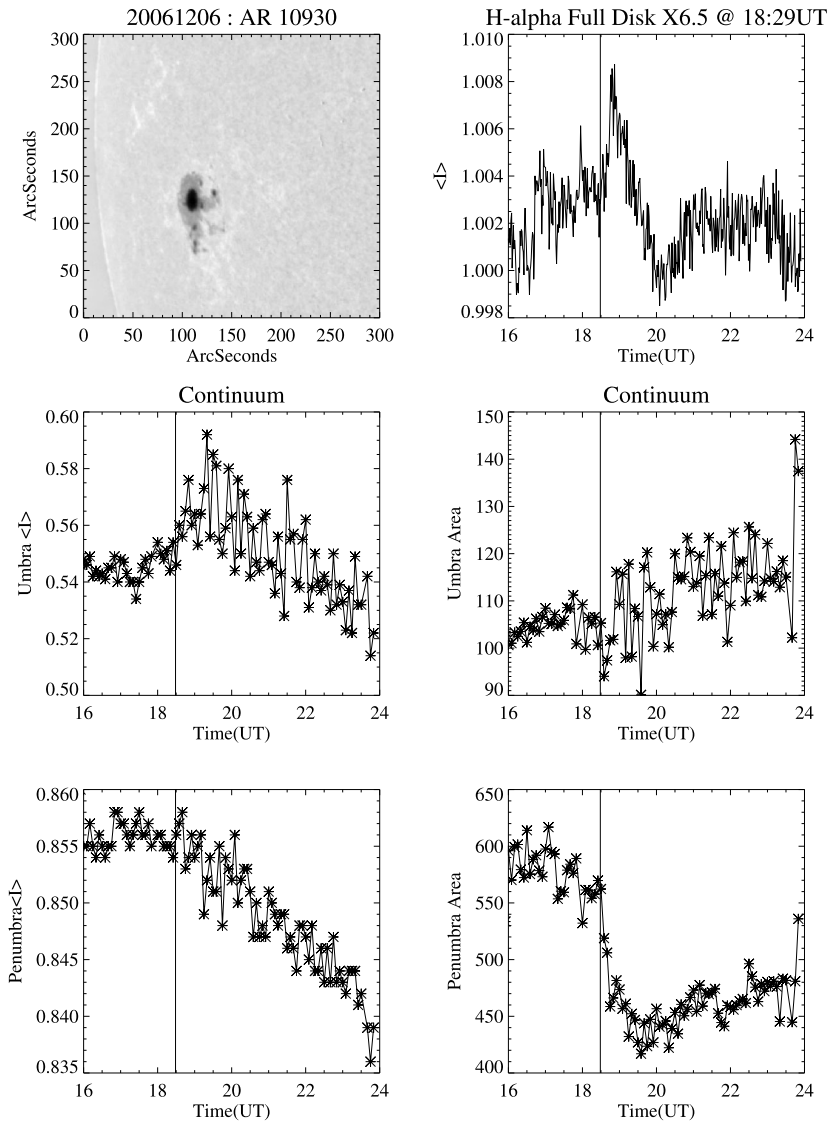
Figure 10 Changes in sunspot penumbral and umbral areas and intensities during the course of a day when a large flare occurred. The panels show the evolution of corresponding areas and intensities for the X6.5 flare of AR 10930 on 06 December 2006. The corresponding mean Hα intensity for the flare, averaged over the active region, is shown in the top-right panel to help identify the start of the flare times. These changes cannot be discerned simply by using a sunspot number.

in vertical umbral fields. Similarly, that the amplitude of the umbral intensity and area are lower before and after the flare can be construed as the suppression of umbral oscillations by stressed magnetic fields. However, such conjectures need to be verified by statistical measures from repeated flaring states.

All of this shows that digital imagery offers the added advantage of measuring intra-day area changes by tracking the rapid changes in solar activity, which can be retroactively

verified. These measures further our understanding of changes in sunspot numbers over shorter timescales than the original once-a-day sunspot-number counts.

4. Discussion and Summary

We have demonstrated the advantages of using consistent digital sunspot images and the insights gained from analyzed sunspot numbers from both sunspot drawings and digital data. We established a coherent comparison of sunspot numbers from both sources, and traced potential errors when comparing international sunspot numbers to recent digital data. We showed that when comparing the pre-2015 ISN data (OLD) to the post-2015 ISN (NEW) data, a consistent-increasing trend of ISN numbers with increased solar activity is obvious when compared with digital imagery data. The OLD and NEW data only differ by a factor of ≈ 0.6. We also showed that intra-day variation of sunspot areas are an alternative to sunspot numbers when digital data are available. We established the conversion metrics for sunspot numbers and sunspot-area measures that were needed in the context of the research.

The merging of digitized continuum images with projection-board drawings as a means of computing Wolf numbers provides a more accurate picture of solar activity. To understand and develop an effective conversion between the two methods under similar conditions, digital images need to be acquired at nearly the same time as the projection-board drawings, at similar, if not identical, locations. This article demonstrates such an effort. A projection-board drawing requires an observer to be sitting at the telescope, drawing and counting sunspots. If no observer is available, the opportunity is lost. Any drawing made is not reviewable, although it may be compared with other observations by other observers elsewhere and at different times. In contrast, a digital image can be reassessed as its analysis can be revisited at any time in the future.

Sunspots can emerge or dissipate at any point in an observing period. In a digital image, faint penumbrae can be frequently identified on a display screen; they persist from image to image, and yet are below the digital (intensity and area) thresholds, to be counted. Hence the automated procedure will miss the spot. Fading in and out, they may or may not be seen on a projected image. The question arises whether to ignore these spots or count them in some way. A researcher needs to be aware that counting sunspots may drastically increase the R-number. One such example was the counting on 13 October 2003, when the southwestern part of the Sun, close to the disk center, showed persistent visual spots. However, the corresponding digital counts showed no such spots because they were below the intensity threshold.

In general, imagery from ISOON detects many more spots and groups than the ISN suggests, but there are many exceptions. Some of the difference will be in the method of counting spots and the identification of penumbrae or umbrae. However, counting umbrae will greatly exaggerate this difference, which can be alleviated by determining minimum thresholds, such as in an area or in darkness, for defining a sunspot.

We also compared ISOON spot counts and NOAA/Space Weather Prediction Center counts, which are immediately available before reconciliation. SWPC uses the USAF's operational SOON telescope network's projection-board drawings in processing the data. Despite better seeing conditions for ISOON (at the high altitude where Sacramento Peak is located), preliminary spot counts reported by NOAA–USAF were consistently greater and often twice as high as those seen with ISOON imagery. For example, from 01 January 2008 to 31 March 2011, there were 609 common observations for ISOON and NOAA reports.

More than ten percent of the time SOON reports registered more than twice the ISOON spot counts.

An image is a means to verify the existence of an active region from an observatory. The method used to assign NOAA active-region numbers can have the effect that active regions may be several days old before they are identified. In addition, we recall that the NOAA active-region number assignment can be temporally outdated by as much as a whole day. In our experience at NSO, numerous one- and two-day events, where new active regions are not numbered, were noted. A one-day event may be understood as that observations at NSO in New Mexico are relatively late in the observing day as compared to other observatories around the world. For NOAA to confirm the existence of an active region, two consecutive observatories in the USAF SOON network must each independently report its existence within a day (one-day), or the same observatory can report the sunspot on two consecutive days (two-days).

In tracking the intra-day variation of solar activity, we demonstrated that sunspot-component measures, such as umbral and penumbral areas and intensities, dramatically change during and after large solar flares. The underlying changes in sunspot areas cannot be reflected in sunspot numbers, which are coarser measures of solar activity on timescales of a day or more. Integrated sunspot areas and irradiance deficits can be diagnostics of alternate measures of solar activity to monitor finer changes. The important point here is that sunspot imagery and quantitative changes are better reflected in measures of component solar activity than in those represented by sunspot-number changes when finer representations of solar activity are considered in the context.

If a network of telescopes were to be constructed, as was planned for ISOON, issues to be resolved would include standardization of wavelength, filter width, and aperture of a candidate telescope. A high-resolution telescope will see very fine spots and can be expected to see more than the human eye. Integrated over time, a more accurate picture of solar activity can be obtained from a telescope with multiple images than from a single observation once a day.

Disclosure of Potential Conflicts of Interest   The authors declare that they have no conflicts of interest.

References

Allen, C.W.: 1991, *Astrophysical Quantities*, Athlone Press, London.

Balasubramaniam, K.S.: 2002, *Astrophys. J.* **575**, 553.

Balasubramaniam, K.S., Pevtsov, A.A.: 2011, In: *Solar Physics and Space Weather Instrumentation*, *Proc. SPIE* **8148**.

Cliver, E.W., Clette, F., Svalgaard, L.F.: 2013, *Cent. Eur. Astrophys. Bull.* **37**, 401.

Györi, L., Baranyi, T., Ludmány, A.: 2010, In: Choudhary, D.P., Strassmeier, K.G. (eds.) *The Physics of Sun and Star Spots Proc. IAU Symp.* **273**, Cambridge University Press, Cambridge, 403. ADS. DOI.

Hathaway, D.H.: 2010, *Living Rev. Solar Phys.* **12**, 4. DOI.

Hathaway, D.H., Wilson, R.M., Reichman, E.J.: 1999, *J. Geophys. Res.* **104**, 22375.

Henry, T.W.: 2015, *Solar ephemeris applications and image analysis*. MS thesis, Texas Tech University, Lubbock, TX.

Hoyt, D.V., Schatten, K.H.: 1998, *Solar Phys.* **179**, 189. ADS. DOI.

Hoyt, D.V., Schatten, K.H., Nesme-Ribes, E.: 1994, *Geophys. Res. Lett.* **21**(18), 2067.

Neidig, F., Henry, T.: 2004, *Comparing sunspot numbers between NSO and ISOON: NSO/Sac peak projection board drawings vs. ISOON semi-automatic procedure*. NSO Internal Technical Document (private communication).

Neidig, D., Wiborg, P., Confer, M., Haas, B., Dunn, R., Balasubramaniam, K.S., Gullixson, C., Craig, D., Kaufman, M., Hull, W., McGraw, R., Henry, T., Rentschler, R., Keller, C., Jones, H., Coulter, R., Gregory, S., Schimming, R., Smaga, B.: 1998, In: Balasubramaniam, K.S., Harvey, J., Rabin, D. (eds.) *Synoptic Solar Physics* **CS-140**, Astron. Soc. Pac., San Francisco, 519.

Pötzi, W., Veronig, A.M., Temmer, M., Baumgartner, D., Freislich, H., Strutzmann, H.: 2016, *Solar Phys.* DOI.

Sivaraman, K.R., Gupta, S.S., Howard, R.F.: 1993, *Solar Phys.* **146**, 27. ADS. DOI.

Smith, H.J., Smith, E.P.: 1963, *Solar Flares*, Macmillan Co., New York.

Tlatov, A.G., Vasil'eva, V.V., Markova, V.V., Otkidychev, P.A.: 2014, *Solar Phys.* **289**, 1403. ADS. DOI.